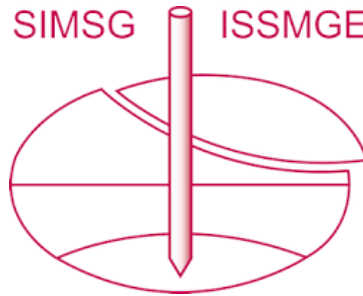


INTERNATIONAL SOCIETY FOR SOIL MECHANICS AND GEOTECHNICAL ENGINEERING



This paper was downloaded from the Online Library of the International Society for Soil Mechanics and Geotechnical Engineering (ISSMGE). The library is available here:

<https://www.issmge.org/publications/online-library>

This is an open-access database that archives thousands of papers published under the Auspices of the ISSMGE and maintained by the Innovation and Development Committee of ISSMGE.

The paper was published in the proceedings of the 10th International Conference on Physical Modelling in Geotechnics and was edited by Moonkyung Chung, Sung-Ryul Kim, Nam-Ryong Kim, Tae-Hyuk Kwon, Heon-Joon Park, Seong-Bae Jo and Jae-Hyun Kim. The conference was held in Daejeon, South Korea from September 19th to September 23rd 2022.

Shaking table tests on seismic response of subway tunnel in silty clay

X. Ma, Z. Wang & N. Feng

Department of Geotechnical Engineering, Tongji University, Shanghai, China

J. Shang

Jinan Rail Transit Group Co.,Ltd, Shandong, China

ABSTRACT: With the development of urbanization, the congestion and inefficiencies of ground transportation become the common problem in large cities, and the development of subway provides an effective solution to this problem. In this paper, the seismic characteristics of the silty clay ground and the embedded tunnel are studied based on shaking table test. The relationship between the input ground motion intensity and the acceleration amplification coefficient in the stratum, the propagation law of seismic wave in the stratum and the variation law of natural vibration frequency and damping ratio of different soil layers with the intensity of seismic wave are obtained. The results show that the tunnel structure vibrates uniformly with the soil at low frequency, while the soil and the structure may be separated under high frequency. With the increase of the input seismic wave intensity, the dividing line between the high frequency and low frequency decreases.

Keywords: tunnel, shaking table test, numerical simulation, modified response displacement method.

1 INTRODUCTION

Metro Engineering is an important part of urban lifeline engineering and plays a very important role in the public transportation of cities. However, in the early days, not enough attention was paid to the seismic research of underground structures such as subways, as they appeared late and in small numbers compared to above-ground structures, most of which had not yet been tested by major earthquakes, and therefore catastrophic damage was not well documented. However, the 1995 Hanshin earthquake in Japan brought about a change in perception. The Hanshin earthquake caused severe damage to a number of underground stations and interdistrict tunnels in Kobe. In the 2008 Wenchuan earthquake in Sichuan, the Chengdu underground under construction was damaged to varying degrees. The above and similar incidents have made the seismic dynamic response of tunnels a hot topic for research. Generally speaking, the methods used to study the seismic dynamic response of tunnels include theoretical analysis, field observations, shaking table model tests and numerical calculations. Among them, shaking table tests take real seismic waves as input, and the structural model on the table can respond according to certain scale factors, thus reproducing the response process in an earthquake. At present, a series of studies have been conducted on the dynamic response of underground structures under the action of seismic forces. Li J, Luzhen et al. (2010) carried out non-uniformly excited and uniformly excited shaking table tests on an

underground utility tunnel. It was found that the acceleration response of the structure was weaker than the surrounding soil under the consistent ground vibration excitation. Also, the maximum stress of the utility tunnel appeared at the right angle, which increased with the increase of PGA, and the section had angular movement. The response of the utility tunnel under the non-uniform ground motion excitation was significantly enhanced compared with that under uniform excitation. Yong Yuan, Haitao Yu et al. (2016) systematically described the model soil configuration, fabrication of model box, node deformation and soil response of immersed tube tunnel under non-uniform excitation based on the research project of seismic dynamic response of Hong Kong-Zhuhai-Macau immersed tube tunnel. The test results showed that the vibration response of the immersed tube tunnel was stronger under non-uniform vibration excitation than that under uniform excitation; certain nodes would produce relatively large tensile deformation under strong seismic action. Zhang Xueming and Yan Weiming et al. (2018) studied the dynamic response characteristics of the immersed tube tunnel structure and its joints by shaking table tests. The test results showed that under consistent excitation, the tunnel and the soil had a relatively consistent overall motion. When the longitudinal traveling wave effect was considered, the soil and the tunnel produced relative slip, while the longitudinal traveling wave effect and its input direction had a large influence on the joint axial force, bending moment and deformation. Also, the traveling

wave effect made the response of the immersed tunnel joint non-uniform.

Due to the specificity of the surrounding rock and seismic waves, the above research results can only be used for reference. In order to have a more accurate understanding of the seismic dynamic response of tunnels and strata under seismic waves and to provide valuable suggestions for the seismic resistance of subways in this region, shaking table tests were carried out for the silty clay layer and its tunnel structure.

2 TEST DESIGN

2.1 Scale factor

In the test, the model soil is silty clay, and the scale factor of soil density is 1. The acceleration scale factor n_a is set at 5. To better reflect the real response of the prototype structure under various intensities, the shaking table noise, the table bearing capacity and even the lifting capacity of the crane are considered.

The scale factors of other parameters are listed in Table 1 below.

Table1 Scale factors.

physical quantity	similarity coefficient	Scale factor
Length l	n_l	0.05
Density ρ	n_ρ	1
Acceleration a	n_a	5
Rigidity G	n_G	0.109
Stress σ	$n_\rho n_a n_l$	0.25
Power F	$n_\rho n_a n_l^3$	0.000625
Strain s	$n_\rho n_a n_l / n_G$	2.29
Displacement d	$n_\rho n_a n_l^2 / n_G$	0.11
Time t	$n_l \left(\frac{n_\rho}{n_G} \right)^{0.5}$	0.15
Frequency f	$\left(\frac{n_G}{n_\rho} \right)^{0.5} / n_l$	6.67
Shear wave velocity v_s	$\left(\frac{n_G}{n_\rho} \right)^{0.5}$	0.33
Speed v	$n_a n_l \left(\frac{n_\rho}{n_G} \right)^{0.5}$	0.75

2.2 Test method

The shaking table produced by MTS company of the United States is used in this test, and the table size is 4m × 4m, the maximum acceleration in one direction is 1.2g. The flexible model box is selected as the test model box, which is cylindrical with a diameter of 3000 mm. In the

model box, 0 ~ 900 mm is silty clay and 900 ~ 1350 mm is sand.

The test input wave is El Centro wave, as shown in Figure 1, and the peak acceleration is 0.143g, 0.41g, 0.6g and 0.918g respectively. The seismic wave is input along the x axis direction and in a increasing order, with corresponds with the working conditions 1 to 4.

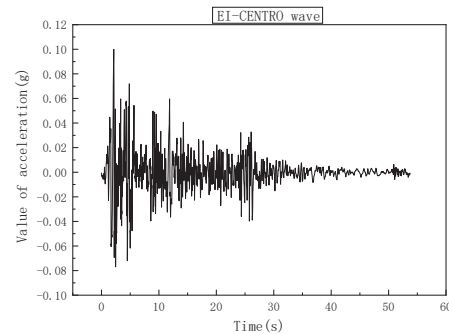


Fig. 1. Time history curve of input wave.

2.3 Layout of measuring points and sensors

The accelerometers are arranged in 3 columns, A, B and C. AC1, AC2, AC9 and AC10 are the accelerometers fixed at the top and bottom of the tunnel vaults, while the others are buried in the ground, as shown in Figures 2 and 3.

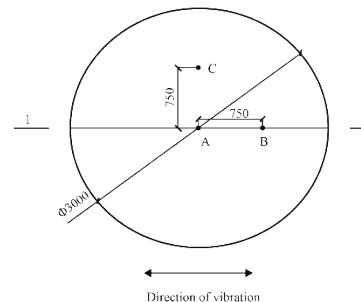


Fig. 2. Top view of the model box(unit: mm).

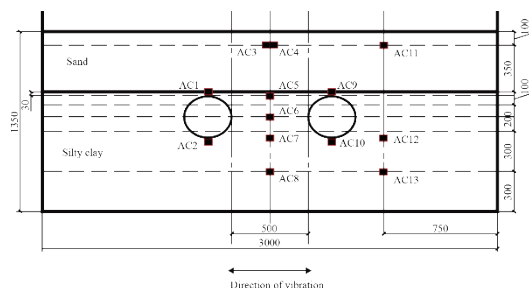


Fig. 3. Longitudinal section 1—1 of model box(unit: mm).

3 TEST RESULTS

3.1 Accelerated amplification factor analysis

The soil layer has an amplifying effect on the acceleration. In order to study the variation law of the

amplifying effect with the burial depth of the soil layer, the acceleration amplification coefficient is used to describe the variation law of acceleration with depth.

The acceleration amplification coefficients at each observation point for each working condition are collated and the results are shown in Figure 4.

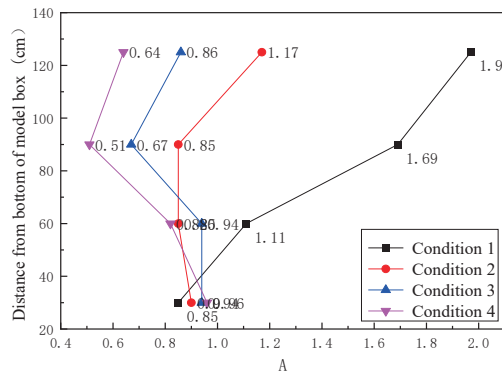


Fig. 4. El-Centro wave amplification coefficients for each operating condition at observation point A.

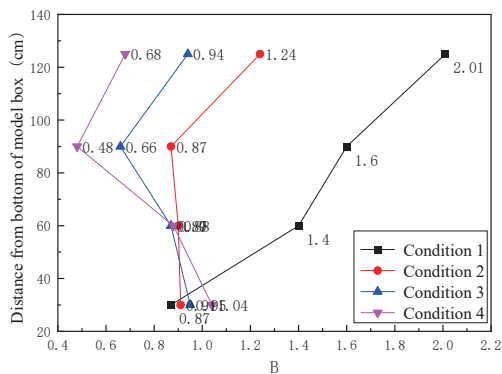


Fig. 5. El-Centro wave amplification coefficients for each operating condition at observation point B.

As shown in Figure 4 and Figure 5, the observations at locations A and B show similar variation pattern for the same condition. In condition 1, the acceleration increases with increasing distance from the seismic input point. For conditions 2, 3 and 4, the acceleration decreases with increasing distance from the bottom of the model box in the range 0-90 cm, and increases with increasing distance from the bottom of the model box in the range 90-135 cm. As the peak acceleration of the input seismic wave increases, the acceleration amplification factor at each observation point tends to decrease.

3.2 Analysis of soil vibration characteristics

Signal processing in the frequency domain tends to be more straightforward and comprehensive than in the time domain. The transfer function is a representation of the site dynamic properties affecting the dynamic response characteristics of the site. The expressions are as follows:

$$T(\omega, h_m) = \frac{G_{XY}(\omega, \omega_m)}{G_{XX}(\omega, \omega)}$$

where $G_{XY}(\omega, \omega_m)$ is the reciprocal power spectrum of the acceleration at measurement point m and the shaker acceleration; $G_{XX}(\omega, \omega)$ is the self-power spectrum of the acceleration at the measurement point; and h_m is the elevation of the measurement point m .

The frequency corresponding to each peak of the transfer function is approximated as the intrinsic frequency of each order, and the damping ratio is calculated by the half-power bandwidth method with the formula:

$$\lambda = \frac{\omega_2 - \omega_1}{2\omega_0}$$

where ω_0 is the natural frequency of the system; ω_1 , ω_2 is 0.707 times the frequency corresponding to the peak value on both sides of the natural frequency, and $\omega_1 < \omega_2$.

The results of the calculations according to the above formula are shown below.

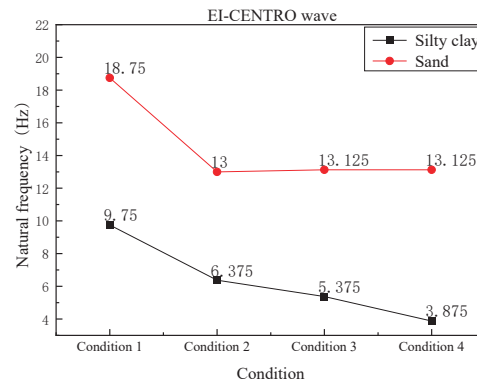


Fig. 6. Natural frequency diagram of different acceleration peak systems.

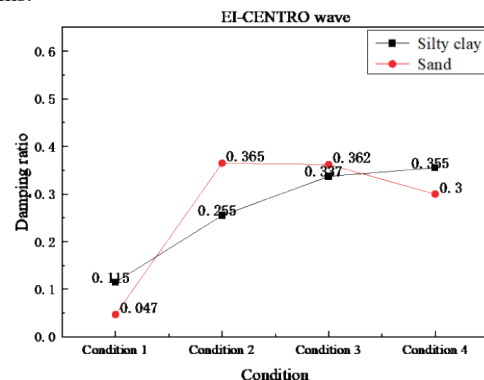


Fig. 7. Damping ratio diagram of different acceleration peak systems.

The results in Figure 6 show that the natural frequency of the soil layer tends to decrease as the peak of the input wave acceleration increases. For the sand

layer, its natural frequency firstly decreases and gradually stabilizes.

The results in Figure 7 show that the damping ratio of the silty clay layer tends to increase with the increase of the input seismic wave intensity in all working conditions. For the sand layer, the damping ratio increase rapidly at the initial stage and gradually decrease.

3.3 Spectrum analysis of tunnel and surrounding strata

The ratios of the acceleration spectra of the top and bottom of the tunnel and the soil layers at the same height for each condition are shown in the Figure 8. In the case of the same seismic wave, there is a critical frequency for the ratio of the tunnel structure to the surrounding soil spectrum. For frequency smaller than this value, the structure and the soil have almost the same vibration amplitude; for frequency larger than this value, the vibration amplitude of the tunnel structure and the soil are not the same. This critical frequency tends to decrease as the peak input acceleration of the shaker increases. It suggests that at low frequencies the tunnel vibrates together with the soil, while at high frequencies the tunnel and the surrounding soil become detached. Also, the separation of soil and the tunnel structure is more obvious under stronger seismic wave.

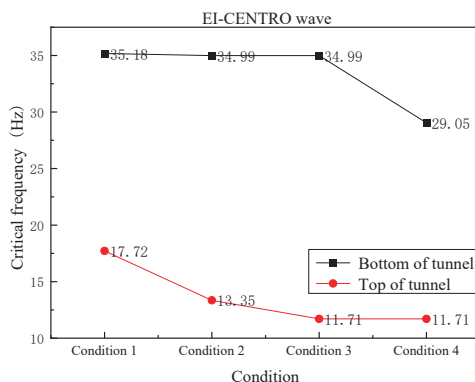


Fig. 8. Acceleration spectrum ratio of tunnel and soil layer with the same buried depth.

4 CONCLUSIONS

In this paper, the dynamic response characteristics of silty clay and the embedded underground structures under the action of seismic forces are studied by shaking table tests, and the following conclusions are drawn.

1. With the increase of the peak acceleration of the input seismic wave, the acceleration amplification coefficient at each observation point shows a decreasing trend.

2. As the intensity of the input seismic wave increases, the natural frequency of the silty clay decreases and the damping ratio increases; the natural frequency of the sand layer firstly decreases and gradually stabilizes, and the damping ratio increase first rapidly at the initial stage

and then gradually decrease.

3. When the seismic wave frequency is lower than a certain value, the tunnel and the soil move together; when the frequency is higher than a certain value, the tunnel and the surrounding soil become detached, and this critical frequency decreases with the increase of the seismic wave intensity.

REFERENCES

- Jiang, Luzhen, Chen. Seismic response of underground utility tunnels: shaking table testing and FEM analysis. *Earthquake Engineering and Engineering Vibration*, 2010, 9(4):555-567.
- Chen J, Shi X, Li J. Shaking table test of utility tunnel under non-uniform earthquake wave excitation. *Soil Dynamics & Earthquake Engineering*, 2010, 30(11):1400-1416.
- Yan X, Yuan J, Yu H, et al. Multi-point shaking table test design for long tunnels under non-uniform seismic loading. *Tunnelling & Underground Space Technology*, 2016, 59:114-126.
- Yong Y, Yu H, Li C, et al. Multi-point shaking table test for long tunnels subjected to non-uniform seismic loadings – Part I: Theory and validation. *Soil Dynamics & Earthquake Engineering*, 2016, Vol. 108, 177-186.
- Yu H, Yuan Y, Xu G, et al. Multi-point shaking table test for long tunnels subjected to non-uniform seismic loadings - part II: Application to the HZM immersed tunnel. *Soil Dynamics & Earthquake Engineering*, 2016, Vol. 108, 187-195.
- Zhang X, Yan W, et al. Seismic performance of immersed tube tunnels considering traveling wave effects: a shaking table array test study. *Vibration and shock*, 2018, 37(2):76-84.